CARS System for Turbulent Flame Measurements

Richard R. Antcliff*
Systems Research Laboratories, Inc., Dayton, Ohio
and
Olin Jarrett Jr.† and R. Clayton Rogers‡
NASA Langley Research Center, Hampton, Virginia

Simultaneous nitrogen number density and rotational-vibrational temperatures were measured in a turbulent diffusion flame with a Coherent Anti-Stokes Raman Scattering (CARS) instrument. The fuel jet was diluted with nitrogen (20% by volume) to allow temperature measurements across the entire jet mixing region. The CARS system incorporated a Neodymium YAG laser, an intensified silicon photodiode array detector and unique dynamic range enhancement methods. Theoretical calculations based on a parabolic Navier-Stokes computer code were compared to the CARS measurements.

Nomenclature

c	= speed of light
C_μ	= viscosity constant
I_i	= intensity
k	= turbulent kinetic energy
l_ϵ	= dissipation length scale
L	= interaction length
N_T	= total number density at temperature T
P_T	= experimentally measured integrated intensity
R_T	= area ratio of the normalized CARS spectrum at 300 K to the normalized spectrum at temperature T
u'	= fluctuating component of the velocity
U	= mean velocity
$\Gamma(v,J)$	= Raman line width
$\delta(v,J)$	= $\omega_R - (\omega_1 - \omega_2)$, deviation from the Raman level
$\Delta(v,J)$	= Boltzman population difference
ϵ	= turbulent dissipation rate
μ_T	= turbulent viscosity
η_3	= refractive index at ω_3
ρ	= local mass density
$d\sigma/dr$	= Raman scattering cross section
$\chi^{(3)}$	= third-order susceptibility
χ_{NR}	= nonresonant susceptibility
ω_i	= frequency

Subscripts

1	= pump beam
2	= probe beam
3	= signal beam
R	= Raman

Introduction

COMPUTATIONAL fluid dynamics (CFD) has been used extensively to model combusting flows. These codes, however, are idealized and correlation with practical measurements has therefore been limited. To help bridge this gap, we have obtained flame property measurements in a simplified burner which can be readily modeled. This paper displays our first attempt to compare our complete measurement system results with theoretical calculations. Analysis of this comparison will be used to refine both CFD modeling techniques and nonintrusive measurements of processes occurring in the supersonic combustion ramjet devices being developed at NASA Langley Research Center. The measurement system being used at NASA Langley is a Coherent Anti-Stokes Raman Scattering (CARS) system. CARS has become a preferred nonintrusive diagnostic technique for application in many hostile combustion environments. These applications include the diagnosis of plasmas,[1,2] internal combustion engines,[3,4] shock tubes,[5,6] and full-scale combustors.[7-9] Nonintrusive optical measurement techniques, although complex, relieve the constraints of physical probe degradation and phenomena interference. CARS also has the advantages of high spatial resolution, high temporal resolution, relatively high conversion efficiency, good collection efficiency resulting from a laser-like signal beam, and high fluorescence discrimination. The computer code used to model the flow and combustion in these studies was an axisymmetric parabolized Navier-Stokes code with equilibrium chemistry and a two-equation turbulence model. This code has been used successfully to model similar burners.[10]

Background

Several excellent reviews include a treatment of the CARS theory[11,12]; therefore, only a brief summary will be presented here. CARS is a nonlinear optical process in which laser beams incident on the sample at frequencies ω_1 and ω_2 interact through the third-order susceptibility of the sample to generate coherent radiation at frequency $\omega_3 = 2\omega_1 - \omega_2$. When the difference in laser frequencies $(\omega_1 - \omega_2)$ becomes close to a Raman resonance in the species studied, the signal output is dramatically enhanced. A plot of this output vs the frequency difference will produce a Raman-like spectrum. This spectrum reflects the vibrational-rotational level populations and is therefore related to the temperature of the sample. Since nitrogen is a major component in air-fed combustion and it has a Q branch that can be easily probed by CARS, it was chosen as the thermometry species. In general, the CARS intensity can be expressed as

$$I_3 = K\frac{\omega_3}{\eta_3} I_1^2 I_2 |\chi^{(3)}|^2 L^2 \qquad (1)$$

Presented as Paper 84-1537 at the AIAA 17th Fluid Dynamics, Plasma Dynamics, and Lasers Conference, Snowmass, Colo., June 25-27, 1984; received Aug. 8, 1984; revision received Jan. 8, 1985.

*Research Chemist, Research Applications Division. Member AIAA.
†Aerospace Engineer, Hypersonic Propulsion Branch, High-Speed Aerodynamics Division.
‡Aerospace Engineer, Hypersonic Propulsion Branch, High Speed Aerodynamics Division. Member AIAA.

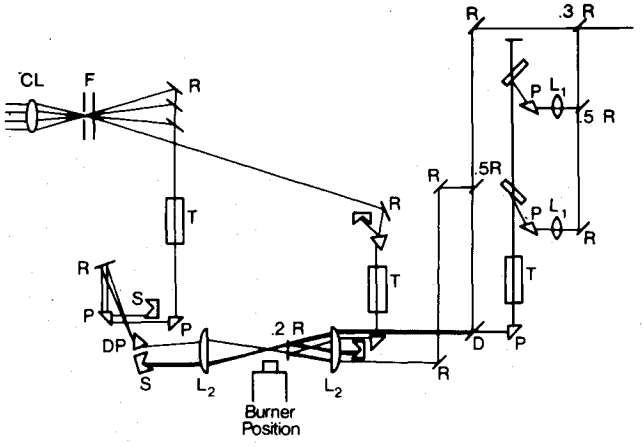

Fig. 1 Schematic of CARS experimental layout. (R) 100% reflector, (L) lens, (P) prism, (D) dichroic mirror, (S) beam stop, (DP) dispersion prism, (T) telescope, (F) filter and iris, (CL) cylindrical lens.

The third-order susceptibility can be expressed as

$$\chi^{(3)} = \frac{2c^4}{k\omega_2{}^4} \sum_{v,J} \frac{N\Delta(v,J)\,(d\sigma/d\Omega)}{\delta(v,J) - i\,\Gamma(v,J)} + \chi_{NR} \qquad (2)$$

Using the values of Rado,[13] a temperature-dependent nonresonant function was calculated from adiabatic flame constituent concentrations.

Apparatus

The CARS system used in these studies is shown in Fig. 1. The pump laser is a pulsed Neodymium YAG laser which produced about 200 mJ at 532 nm in a 10-ns pulse. This laser was also used to pump a broadband dye laser centered about 606.3 nm. Interaction of the doubled Neodymium YAG laser and the broadband dye laser generated the complete CARS nitrogen Q-branch spectrum in a 10-ns laser shot. This short laser pulse produced the high temporal resolution required in turbulent environments. The dye laser output was compared with neon discharge lines to ensure its frequency integrity. To obtain high spatial resolution and optimum phase matching conditions, the optical system was arranged in the BOXCARS configuration.[14] The three input beams were crossed and focused by a 3-in. diam, 30-cm focal length, plano-convex lens. This configuration resulted in an interaction length of approximately 1 mm. The signal generated in the sample volume exited nearly colinearly with one of the ω_1 beams and was therefore directed through a dispersion prism.

To obtain nitrogen number density, a reference signal was necessary to monitor the fluctuation in the CARS generation efficiency. This efficiency is a function of laser power, interaction length, and other experimental variables. The referencing scheme used by Goss et al.[15] which utilizes a retroreflecting splitter, was employed. In this system a 20% broadband reflector was positioned between the focusing lens and the focal position. This reflector produced a second focus in ambient air, which was used for the reference signal.

The detector used was an EG&G PAR 1420 intensified silicon photo-diode array (ISPD) controlled by an EG&G PAR 1218 controller. Data acquisition and scanning of this detector were controlled by a 16-bit MODCOMP computer.[16] This computer allowed a large volume of data to be obtained at a 10-Hz rate. The large volume of data was necessary to obtain reasonable probability distribution functions of temperature at many locations in the flame. The ISPD has been studied extensively to obtain acceptable operating conditions and ascertain its usable dynamic range.[17] It has been found that when the spherical lens normally employed to focus the CARS signal onto the monochrometer entrance was replaced with a cylindrical lens, the linear range of the detector was increased by a factor of five. This increased range was still insufficient, however, to cover the entire signal intensity range encountered under turbulent flame conditions. A 10^5 variation in signal intensity results from the squared dependency on number density. For this reason, an additional dynamic range extension similar to that used by Goss et al.[18] was employed. A series of beam splitters was used to image fractions (~1,20,79%) of the signal beam simultaneously onto the detector. In addition to these three signals, the reference signal was also imaged on the ISPD. To accommodate these signals, the monochrometer entrance slits were rotated horizontally and the signals were positioned side by side; this allowed the data and reference signals to be recorded simultaneously.

The system was calibrated with a premixed flat flame burner. This burner has been previously studied and found to have a well-behaved temperature profile.[19] The system was found to have an intrinsic temperature standard deviation of approximately 5% and an intrinsic concentration standard deviation of approximately 10%. Theoretical temperatures and densities calculated from the burner flow conditions fall well within these limits, which indicates the accuracy of the system. Therefore, deviations larger than these in this study were caused by flame structure. The effects of turbulence on the laser beams, which include beam steering, beam defocusing, and focal shifting, can cause density errors when high refractive index gradients are present.[18] These effects have been assumed negligible in this study.

The burner used in the present studies was a subsonic diffusion flame device consisting of two coaxial tubes. The inner tube, which contained the fuel, had a 4.7-mm i.d.; the outer tube had a 25.4-mm i.d. and contained air. The outer wall of the inner tube was tapered near the tip from an o.d. of 6.4 mm to a base lip thickness of 0.51 mm. The length of the burner was approximately 45 cm.

Predictions of Subsonic Coaxial Jet Mixing

Calculations of the flowfield produced by the mixing and combustion of subsonic hydrogen/nitrogen and air in a coaxial jet arrangement have been made with a parabolic flow computer code.[20] This code solves the parabolized Navier-Stokes equation using a marching finite-difference algorithm and includes the two-equation turbulence model ($k = \epsilon$). Combustion is modeled by hydrogen-oxygen equilibrium chemistry with nitrogen inert.

Input to the code consisted of profiles of velocity, fuel mass fraction, turbulent kinetic energy, static temperature, and static pressure at the initial station located 0.01 fuel jet diam downstream of the jet exit plane. Calculations of turbulent diffusion flames with codes of this type have been shown to be very sensitive to the initial conditions (e.g., Ref. 20), particularly velocity and turbulence quantities. To model the burner flow best, initial velocity and turbulence intensity profiles were obtained from a series of cold flow tests using a standard hot-wire aneometer probe. The hot-wire data were collected with air in both the fuel and air jet. Typical profiles near the exit of the burner apparatus are presented in Fig. 2. A total of 250 data points at 0.127-mm intervals are represented by each of the profiles. The velocity values were calculated from the hot-wire data using a linearized model. A good discussion of the hot-wire techniques is presented by Hinze.[21] Exit plane velocity data of the center jet with hydrogen injection showed a velocity profile shape identical to that for the air jet in Fig. 2. As initial profiles input to the computer code, the velocity profile was normalized relative to the centerline value. In calculating the diffusion flame flow, the centerline value was adjusted in magnitude to obtain jet mass flow rates equal to experimentally measured values. Typically the centerline velocity was 136 m/s in the fuel jet; nominal velocity in the annular air jet was 15.5 m/s.

Due to experimental considerations, the center jet (fuel) was a uniform mixture of 20% nitrogen and 80% hydrogen by

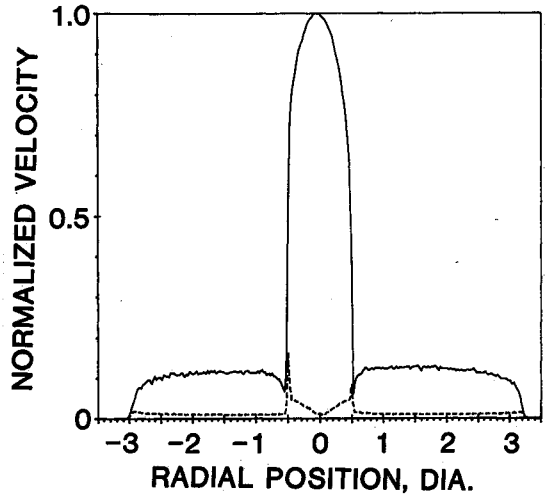

Fig. 2 Hot-wire velocity profile across a diameter of the coaxial burner using air to simulate all gas flows. (Solid line) local average velocity; (dotted line) local turbulent velocity.

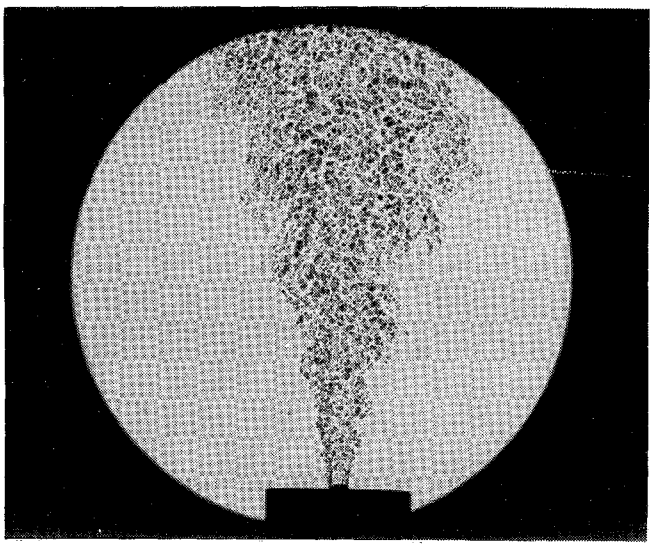

Fig. 3 Shadowgraph of turbulent diffusion flame.

volume (mass fractions of 0.776 N_2, 0.224 H_2). The initial profile of the fuel mixture was assumed to be 100% within the center jet tube, with a linear decrease to zero over the jet tube lip thickness (0.51 mm). Initial profiles of static temperature and pressure were assumed uniform over both jets at 300 K and 1 atm, respectively. The initial turbulence was obtained by the method used in Ref. 20. Since the turbulence intensity (u'/U) profile was known from the hot-wire data shown in Fig. 2, the initial turbulent kinetic energy k was obtained, by definition, from

$$k = \tfrac{1}{2}(u'/U)^2 \tag{3}$$

The magnitude of the dissipation rate was then obtained as

$$\epsilon = c_\mu k^{3/2}/l_\epsilon \tag{4}$$

Based on comparisons of predicted and measured centerline velocity data, the length scale was chosen as 0.025 fuel jet diam. This quantity is approximately one-fifth of the lip thickness of the hydrogen jet tube. This value is typically 0.1 mm compared with a laser interaction length of ~1.0 mm. The turbulent viscosity is given by

$$\mu_T = \rho c_\mu k^2/\epsilon \tag{5}$$

where ρ is the local mass density.

Based on these assumptions and initial data, the mixing and reacting flowfield of the coaxial hydrogen/nitrogen in air jets was computed. Local chemical equilibrium was used to compute the burning in the diffusion flame. Equilibrium chemistry assumes that the local mixture reacts instantaneously to an equilibrium mixture of products H, O, H_2O, OH, O_2, and H_2 with N_2 assumed inert. This model for the chemical reaction is an ideal case since, in reality, the chemical reactions proceed at a finite rate. In addition, the present computer code does not include any effects of the turbulence in the chemical reaction. For these reasons, the computed results would be expected to overpredict the heat release in the mixing region of the flow resulting in higher temperatures and more rapid spreading. However, research on the interactive effects of turbulence on chemical reaction rates has recently been reported.[22] In this reference, probability density functions are used to account for fluctuations in temperatures and species concentrations on chemical reaction rates. This refinement of the turbulence-chemistry model is currently being included in the computer code. The present and future data will provide a good case for testing the probability density function approach.

Experimental

For this work the burner was operated with nominal velocities of 100 m/s in the central jet and 15.5 m/s in the outside annular air jet, which corresponds to metered mass flow rates of 100 and 575 standard liters per minute (SLM) in the central and annular jets, respectively.

In some preliminary experiments, pure hydrogen was used in the central jet. However, since nitrogen was used as the thermometry species, accurate temperature measurements could not be made near the jet exit because of insufficient nitrogen in the potential core of the flame. This lack of nitrogen produced a large increase in the relative nonresonant signal disturbing the CARS band shape. This problem has recently been addressed by Hall and Boedeker.[23] Their approach was to treat the nonresonant susceptibility as a fitting parameter in the data reduction. We chose, alternatively, to introduce a known quantity of nitrogen into the central fuel jet. For the measurements included in this paper, a mixture of 20% nitrogen and 80% hydrogen by volume was used as noted above. Test conditions were established by using an external flame to light the fuel jet at a reduced air-jet flow. Air flow was then brought up to the desired test conditions while maintaining an attached flame. The Reynolds number of the central jet gas, based on the fuel tube jet diameter was approximately 8000.

A shadowgraph of this burner operated under similar conditions is shown in Fig. 3. This figure illustrates the turbulent nature of the flame system studied. Motion shadowgraphs indicate large periodic vortex structures in the shear layer and smaller-scale shear-induced turbulence.

Data Reduction

To obtain temperature information from the CARS data, the experimental data were compared with theoretical CARS spectra. These spectra were precalculated at 20-deg increments and stored on a computer disk. The experimental data were retrieved and corrected with a background data scan and the detector response function. The computer then selected the largest unsaturated signal of the three simultaneously recorded CARS signals. A nonlinear least-squares procedure[24] was then used to compare the measured data with the precalculated theoretical spectra.

Once the temperature had been obtained, the concentration was determined from the integrated area of the CARS signal. The nitrogen number density has been shown to be[15]

$$N_T = N_{300}[(R_T P_T)/P_{300}]^4 \tag{6}$$

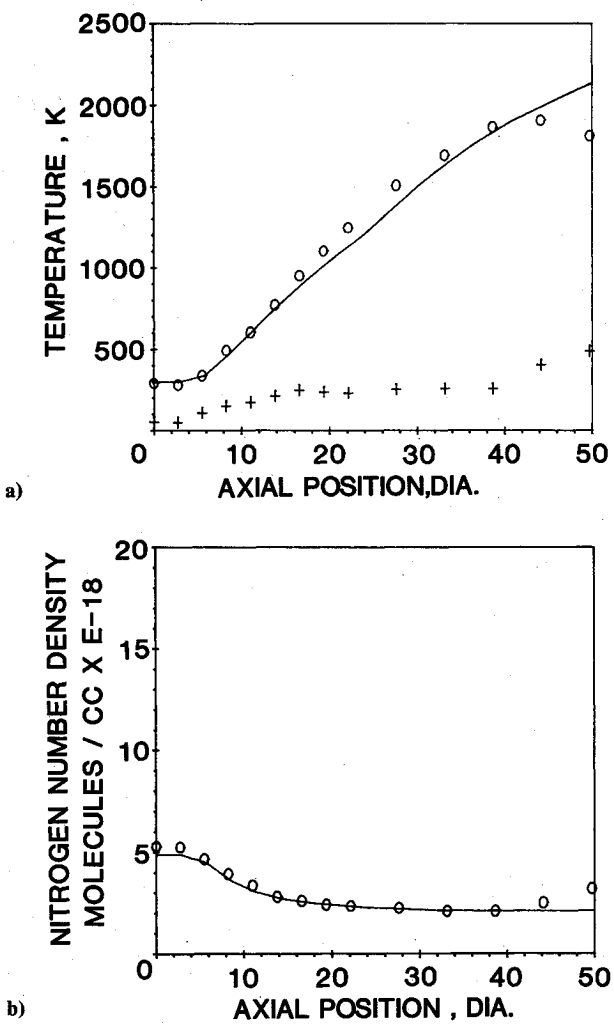

Fig. 4 Axial profile. (Circles) CARS experimental data; (solid line) theoretical calculation: a) temperature profile, plus symbols are the value of one standard deviation; b) nitrogen number density profile.

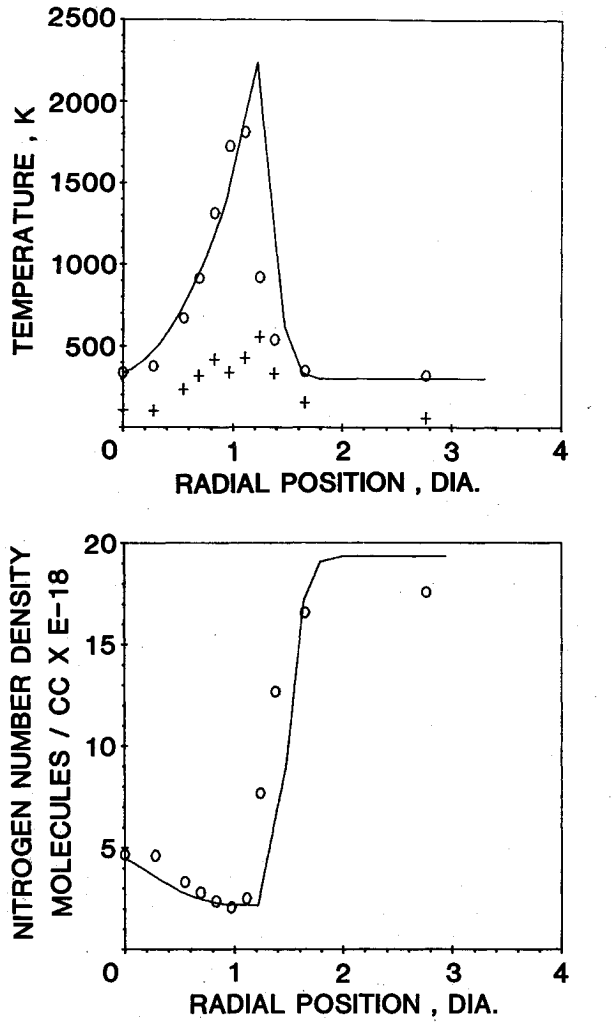

Fig. 5 Radial profile (5.4 diam downstream). (Circles) CARS experimental data; (solid line) theoretical calculation: a) temperature profile, plus symbols are the value of one standard deviation; b) nitrogen number density profile.

Approximately 2 s were required for each inversion. Two hundred shots were taken at each measurement location. The inverted temperatures and number densities were then used to construct probability distribution functions, from which the mean and standard deviation were obtained.

Results

Figure 4a shows the temperature distribution along the centerline obtained in the subsonic diffusion burner. The CARS value used for display at each location is the mean of the 200 measurements. Agreement between the mean CARS values and the calculated values is remarkably good, especially below 40 diam. Beyond this point the CARS data tend to level off, while the calculated data continue to increase. Notice also that the turbulence intensity (indicated by the standard deviation values) is relatively flat until it reaches the 40-diam point, at which time it increases. Figure 4b displays the nitrogen number density correlation. Again the agreement is quite good. Note that the maximum nitrogen density occurs at the exit plane of the fuel jet. At this point the nitrogen density should equal 20% N_2 in the N_2/H_2 mixture at 300 K and 1 atm. As indicated by the calculated data, this corresponds to $\sim 4.9 \times 10^{+18}$ molecules/cc.

Figures 5 and 6 display two radial profiles at 5.4 and 21.6 fuel jet diam downstream, respectively. The temperature increases from ambient radially until the interaction layer is reached, at which point the maximum temperature is reached. It then decreases again to ambient. The radial position of maximum temperature increases with downstream distance and the flame broadens. The standard deviation values exhibit a maximum at the maximum temperature gradient, as expected. The number density at the 5.4-diam station decreases from the 20% value to the fully combusted value and then rises again to the ambient density ($1.92 \times 10^{+18}$ molecules/cc). At the 21.6-diam station, the seeded nitrogen has become fully mixed and the nitrogen density remains constant until the interaction layer is passed.

The most obvious characteristic of these data is that the calculated data are predicting a more rapid spreading of the flame than the CARS data. The spreading predicted is typical of the results obtained when chemistry and turbulence are mutually exclusive in the solution.[22] Including the effects of turbulent fluctuations on the chemistry and using a finite-rate reaction model can have a pronounced effect on the prediction of mixing. The present calculations are only a first attempt at modeling the flame. Subsequent modeling efforts are planned to include the effects of turbulence-chemistry interaction. The figures do, however, show the expected trends in temperature and number density.

Summary

A sophisticated CARS system has been coupled with CFD calculations for investigation of turbulent flames. The CARS system is a broadband planar BOXCARS arrangement using a Nd:YAG as the pump laser. A large dynamic range was achieved by using a combination of three beam splitters and a cylindrical signal focusing lens. Preliminary theoretical

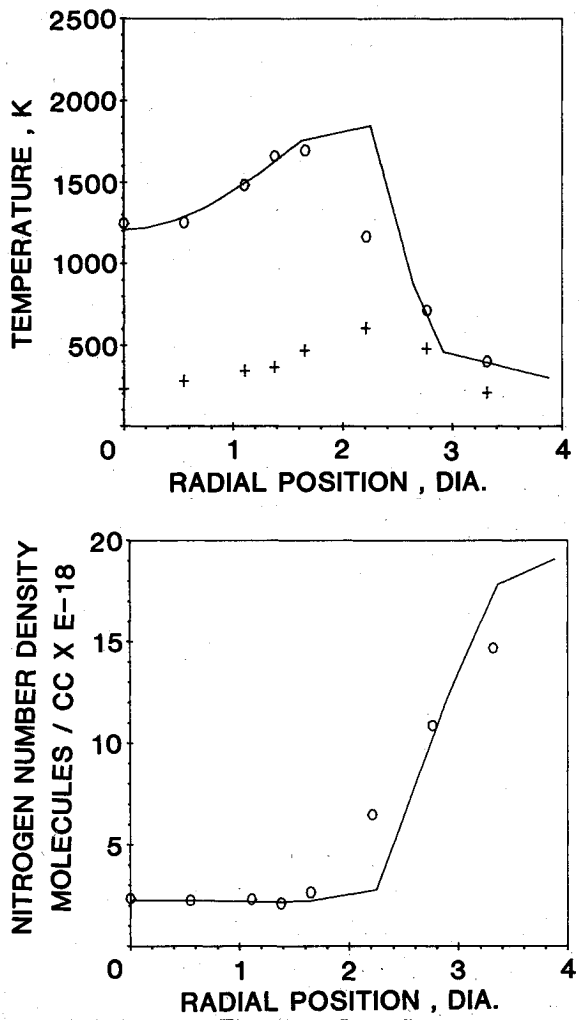

Fig. 6 Radial profile (21.6 diam downstream). (Circles) CARS experimental data; (solid line) theoretical calculation: a) temperature profile, plus symbols are the value of one standard deviation; b) nitrogen number density profile.

calculations were generated using a parabolized Navier-Stokes approximation. The correlation between these techniques is reasonable; however, these calculations predict a faster spreading of the flame than is indicated by the experimental data. More elaborate calculations including a finite-rate chemistry and models that include coupling between turbulence and reaction are currently being studied to improve this correlation.

References

[1]Hata, N., Matsuda, A., Tanaka, K., Kajiyama, K., Maro, N., and Sajiki, K., "Detection of Neutral Species in Silane Plasma Using Coherent Anti-Stokes Raman Spectroscopy," *Japanese Journal of Applied Physics*, Vol. 22, 1983, pp. L1-L3.

[2]Taran, J. P. and Pealet, M., "Practical CARS Temperature Measurements," *6th Symposium on Temperature, Its Measurement and Control in Science and Industry*, Office National d'Etudes et de Recherches Aerospatiales, Toulouse, France, TP No. 1982-6, March 1982.

[3]Alessandretti, G. C. and Violino, P., "Thermometry by CARS in an Automobile Engine," *Journal of Physics D: Applied Physics*, Vol. 16, 1983, pp. 1583-1594.

[4]Klick, D., Marko, K. A., and Rimai, L., "Broadband Single-Pulse CARS Spectra in a Fired Internal Combustion Engine," *Applied Optics*, Vol. 20, 1981, pp. 1178-1181.

[5]Matsumoto, Y., Matsui, H., and Asaba, T., "Measurement of CARS Intensity in Hydrogen Molecule Behind Shock Waves," *Transactions of the Japan Society for Aeronautical and Space Sciences*, Vol. 26, No. 73, Nov. 1983, pp. 131-140.

[6]Knapp, K. and Hindelang, F. J., "Measurement of Temperatures in a Shock Tube by Coherent Anti-Stokes Raman Spectroscopy (CARS)," *Proceedings of 13th International Symposium on Shock Tubes and Waves*, State University of New York Press, Albany, N. Y., July 1981, pp. 132-140.

[7]Goss, L. P., MacDonald, B. G., Trump, D. D., and Switzer, G. L., "CARS Thermometry and N_2 Number Density Measurements in a Turbulent Diffusion Flame," AIAA Paper 83-1480, June 1983.

[8]Eckbreth, A. C., Dobbs, G. M., Stufflebeam, J. H., and Tellex, P. A., "CARS Temperature and Species Measurements in Augmented Jet Engine Exhausts," AIAA Paper 83-1294, June 1983.

[9]Farrario, A., Garbi, M., and Malvicini, C., "Real Time CARS Spectroscopy in a Semi-Industrial Furnace," Centro Inforncizioni Studi Esperienze (CISE), Milan, Italy, Report 2042, 1983.

[10]Spalding, D. B., Launder, B. E., Morse, A. P., and Maples, G., "Combustion of Hydrogen-Air Jets in Local Chemical Equilibrium (A Guide to the Charnal Computer Program)," NASA CR-2407, June 1974.

[11]Hudson, B. S., "Coherent Anti-Stokes Raman Spectroscopy," *American Chemical Society Symposium Series*, Vol. 85, 1978, pp. 171-192.

[12]Tolles, W. M., Nibler, J. W., MacDonald, J. R., and Harvey, A. B., "A Review of the Theory and Application of Coherent Anti-Stokes Raman Spectroscopy (CARS)," *Applied Spectroscopy*, Vol. 31, No. 4, July/Aug. 1977, pp. 253-271.

[13]Rado, W. G., "The Nonlinear Third Order Dielectric Susceptibility Coefficients of Gases and Optical Third Harmonic Generation," *Applied Physics Letters*, Vol. 11, No. 4, Aug. 1967, pp. 123-125.

[14]Eckbreth, A. C., "BOXCARS: Crossed-Beam Phase-Matched CARS Generation in Gases," *Applied Physics Letters*, Vol. 32, No. 7, April 1978, pp. 421-423.

[15]Goss, L. P., Switzer, G. L., and Schreiber, P. W., "Flame Studies with the Coherent Anti-Stokes Raman Spectroscopy Technique," *Journal of Energy*, Vol. 7, No. 5, May 1983, pp. 389-395.

[16]Posenau, J. H. and Antcliff, R. R., "Multichannel Detector Control with a MODCOMP Computer," Kentron International, Inc., Paper presented at the Americas Annual MUSE Meeting, Ft. Lauderdale, Fla., Dec. 1983.

[17]Antcliff, R. R., Hillard, M. E., and Jarrett, O. Jr., "Intensified Silicon Photodiode Array Linearity: Application to Coherent Anti-Stokes Raman Spectroscopy," *Applied Optics*, Vol. 23, No. 14, July 15, 1984, pp. 2369-2375.

[18]Goss, L. P., Trump, D. D., MacDonald, B. G., and Switzer, G. L., "10-Hz Coherent Anti-Stokes Raman Spectroscopy Apparatus for Turbulent Combustion Studies," *Review of Scientific Instruments*, Vol. 54, No. 5, May 1983, pp. 563-571.

[19]Antcliff, R. R. and Jarrett, O. Jr., "Comparison of CARS Combustion Temperatures with Standard Techniques," AIAA Paper 83-1482, June 1983.

[20]Evans, John, S., Schexnayder, C. L. Jr., and Beach, H. L. Jr., "Application of a Two-Dimensional Parabolic Computer Program to Prediction of Turbulent Reacting Flows," NASA TP-1169, March 1978.

[21]Hinze, J. O., *Turbulence—An Introduction to Its Mechanism and Theory*, McGraw-Hill, New York, 1959.

[22]Chinitz, W. and Evans, J. S., "A Model for Reaction Rate in Turbulent Reacting Flows," NASA TM 85746, May 1984.

[23]Hall, R. T. and Boedeker, L. R., "CARS Thermometry in Fuel-Rich Combustion Zones," *Applied Optics*, Vol. 23, No. 9, May 1, 1984, pp. 1340-1346.

[24]Kim, H., "Computer Programming in Physical Chemistry Laboratory: Least Squares Analysis," *Journal of Chemical Education*, Vol. 47, Feb. 1970, pp. 120-122.